Identification and Kinetic Study of the Peroxymalonyl Radical in the Aerobic Oxidation of Malonic Acid by Cerium(IV)

B. Neumann and S. C. Müller

Max-Planck-Institut für molekulare Physiologie Rheinlanddamm 201, D-44139 Dortmund, Germany

M. J. B. Hauser, O. Steinbock, R. H. Simoyi, and N. S. Dalal*

Department of Chemistry, West Virginia University Morgantown, West Virginia 26506-6045

Received December 5, 1994

There is currently considerable interest in definitive characterization of organoperoxy radicals in aqueous media because these radicals seem to play key roles in many chemical (e.g., autoxidation) and biochemical (e.g., lipid peroxidation) reactions.[1] In this communication we present electron paramagnetic resonance (EPR) evidence for the formation of the peroxymalonyl radical (MAOO•) in the aerobic oxidation of malonic acid (MA) by ceric ions. This work was undertaken for the following reasons: First, the peroxymalonyl radical is expected to yield a simple EPR spectrum, a doublet due to hyperfine interaction with only a single proton. Second, deuterium labeling should be feasible and should provide an important help in the structural identification. Third, the system Ce(IV) and malonic acid is an integral part of the Belousov−Zhabotinsky (BZ) reaction. The chemical mechanism of the BZ reaction[2] has been the subject of numerous investigations, because the chemical and physical processes related to this reaction have afforded easy ways of understanding the basis of many nonlinear phenomena, including oscillating reactions, chaos, and spatiotemporal self-organization.[3] However, despite intense efforts over the past three decades, the detailed mechanism of the BZ reaction is still not fully understood. One of the largely unclear aspects concerns the role of molecular oxygen in the overall reaction mechanism. Proposed models generally postulate that oxygen participates via a chain reaction in which the MAOO• is a key intermediate.[4−6] However, these models have not been verified experimentally, especially with regard to the existence of the MAOO• radical. We present results of kinetic investigations on the MAOO• and the malonyl radical (MA•) in oxygen-saturated solutions.

EPR measurements were performed utilizing a Bruker ER200D X-band (9.5 GHz) EPR spectrometer. The reactants were delivered by a peristaltic pump (Gilson Miniplus3) to a quartz flat cell equipped with a T-shaped mixing device. The quartz flow cell (Wilmad WG-804-Q) was mounted in the EPR resonator cavity and had an active and a dead volume of 125 μL and <50 μL, respectively. The flow rates were varied from 3 to 17 mL/min. Radical concentrations and g values were determined utilizing the stable radicals 4-hydroxy-2,2,6,6-tetramethylpiperidine-*N*-oxyl and 1,1-diphenyl-2-picrylhydrazyl (Aldrich) as standards. For measurements of the deuterated system, the entire reaction was carried out using deuterated compounds, i.e., D_2O, D_2SO_4, and perdeuterated malonic acid (Sigma).

Figure 1a shows an EPR spectrum obtained from the reaction between Ce(IV) and malonic acid in 1 M H_2SO_4 after equilibration of the solutions with oxygen. The spectrum consists of two sets of doublets: The high-field doublet has a g value of 2.0037 ± 0.0002 and a proton hyperfine coupling a_H = 20.3 ± 0.1 G, which corresponds to the reported values of the malonyl radical (MA•).[7−9] The broader doublet on the low-field side (g = 2.0150 ± 0.0002, a_H = 4.4 ± 0.2 G) is assigned to the peroxymalonyl radical, because (i) the signal appears exclusively in the presence of oxygen and shows no saturation at high microwave powers; (ii) the g value (2.0150) being significantly larger than 2.0037 is a strong indication of spin density on oxygen atoms and compares well with those of known peroxyalkyl radicals ($2.011 \leq g \leq 2.016$),[10] and (iii) the doublet collapses into a singlet at the same g value when the deuterated analogs are used (Figure 1c), because the expected deuteron hyperfine coupling (0.5 G) is too small to be resolved due to the large (4 G peak-to-peak) inherent line width of MAOO•.

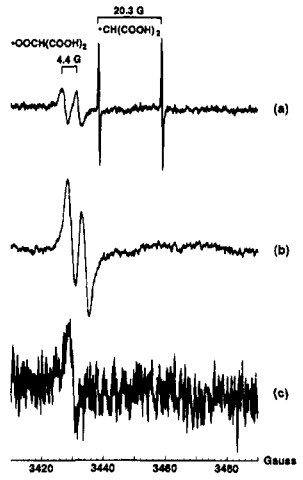

Figure 1. EPR spectrum observed from the reaction of Ce(IV) with MA under oxygen atmosphere. Chemical conditions: 3.3×10^{-3} M Ce(IV), 0.5 M MA, 1 M H_2SO_4. EPR settings: (a) microwave power 11 mW, modulation amplitude 2 G, and (b) microwave power 110 mW, modulation amplitude 8 G. (c) EPR spectrum of deuterioperoxymalonyl radical obtained under the same conditions as spectrum a.

Figure 1b reveals that the EPR settings for optimal measurements of the MAOO• radical are significantly different from those of the MA• radical. The presented spectrum (Figure 1b) was obtained at 110 mW microwave power and 8 G modulation amplitude. Due to the large modulation amplitude and to saturation of the carbon-centered malonyl radical at high microwave power, the spectrum consists of only the MAOO• signal.

The decay kinetics of the peroxymalonyl and the malonyl radicals were measured experimentally and compared with simulations (Figure 2). We performed kinetic measurements under stopped-flow conditions using the EPR setup described above. The experimental concentrations were as follows: 7×10^{-3} M Ce(IV) ($(NH_4)_4Ce(SO_4)_4$, Fluka), 0.5 M malonic acid (doubly recrystallized from acetone) in 1 M H_2SO_4. Separate stock solutions of Ce(IV) and MA in 1 M H_2SO_4 (containing twice the concentrations of MA and Ce(IV) as in the flow cell) were equilibrated with oxygen for at least 20 min prior to the start of the experiment and kept under this condition during the measurements. We estimated the oxygen concentration to be 1×10^{-3} M. All measurements were carried out at room temperature (25 ± 2 °C).

(1) von Sonntag, C.; Schuchmann, H.-P. *Angew. Chem., Int. Ed. Engl.* **1991**, *30*, 1229−1253.
(2) Field, R. J., Burger, M., Eds. *Oscillations and Traveling Waves in Chemical Systems*; Wiley-Interscience: New York, 1985.
(3) Swinney, H. L., Krinsky, V. I., Eds. *Waves and Patterns in Chemical and Biological Media*; North-Holland: Amsterdam, 1991.
(4) Zhabotinsky, A. M.; Müller, S. C.; Hess, B. *Physica D* **1991**, *49*, 47−51.
(5) Barkin, S.; Bixon, M.; Noyes, R. M.; Bar Eli, K. *Int. J. Chem. Kinet.* **1978**, *10*, 619−636.
(6) Zhabotinsky, A. M.; Györgyi, L.; Dolník, M.; Epstein, I. R. *J. Phys. Chem.* **1994**, *98*, 7981−7990. Treindl, L.; Fabian, P. *Collect. Czech. Chem. Commun.* **1980**, *45*, 1168−1172.
(7) Amjad, Z.; McAuley, A. *J. Chem. Soc., Dalton Trans.* **1977**, 304−308. Eiben, K.; Fessenden, R. W. *J. Phys. Chem.* **1971**, *75*, 1186−1201.
(8) Brusa, M. A.; Perissinotti, L. J.; Colussi, A. J. *J. Phys. Chem.* **1985**, *89*, 1572−1574.
(9) Försterling, H.-D.; Noszticzius, Z. *J. Phys. Chem.* **1989**, *93*, 2740−2748.
(10) Howard, J. A. In *Landolt-Börnstein, Neue Serie, II/9c2*; Fischer, H., Hellwege, K.-H., Eds.; Springer: Berlin, 1979; pp 5−28. Howard, J. A. In *Landolt-Börnstein, Neue Serie, II/17e*; Fischer, H., Ed.; Springer: Berlin, 1988; pp 5−35.

0002-7863/95/1517-6372$09.00/0

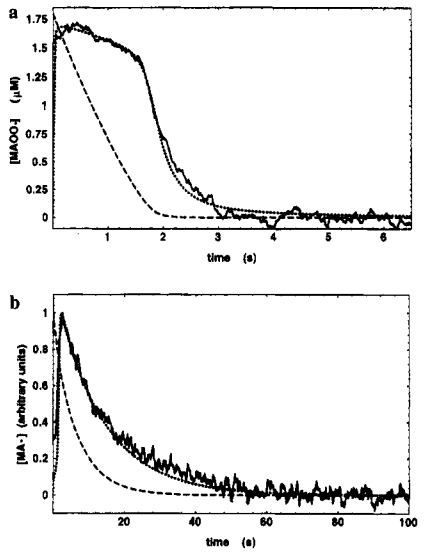

Figure 2. (a) Solid line: experimental data of the peroxymalonyl radical kinetics. Conditions: 7×10^{-3} M Ce(IV), 0.5 M MA, 1 M H_2SO_4. EPR settings: microwave power 110 mW, modulation amplitude 8 G. Dotted line: calculated kinetics of the peroxymalonyl radical. Dashed line: calculated decay of the oxygen concentration. (b) Solid line: experimental data of the malonyl radical kinetics. Chemical conditions: same as in part a. EPR settings: microwave power 11 mW, modulation amplitude 4 G. Dotted line: calculated kinetics of the malonyl radical. Dashed line: calculated kinetics of the Ce(IV) decay.

We propose the following simple reaction mechanism, which serves as basis for modeling our experimental results:

anaerobic part

$$\text{Ce(IV)} + \text{MA} \rightarrow \text{Ce(III)} + \text{MA}^\bullet + \text{H}^+ \quad (1)$$

$$\text{MA}^\bullet + \text{MA}^\bullet \rightarrow \text{ETA} \quad (2)$$

aerobic part

$$\text{MA}^\bullet + \text{O}_2 \rightarrow \text{MAOO}^\bullet \quad (3)$$

$$\text{MAOO}^\bullet + \text{MA} \rightarrow \text{MA}^\bullet + \text{MAOOH} \quad (4)$$

$$\text{Ce(IV)} + \text{MAOOH} \rightarrow \text{Ce(III)} + \text{MAOO}^\bullet + \text{H}^+ \quad (5)$$

$$\text{MAOO}^\bullet + \text{MAOO}^\bullet \rightarrow \text{TA} + \text{MOA} + \text{O}_2 \quad (6)$$

$$\text{MAOOH} \rightarrow \text{P} \quad (7)$$

rate constants and error intervals ($M^{-1}\,s^{-1}$; except s^{-1} for k_7)

$k_1 = 0.3 \quad (0.275 \le k_1 \le 0.31)$

$k_2 = 4.2 \times 10^8 \quad (3.0 \times 10^8 \le k_2 \le 1.2 \times 10^9)$

$k_3 = 1.7 \times 10^7 \quad (1.0 \times 10^7 \le k_3 \le 2.0 \times 10^7)$

$k_4 = 300 \quad (210 \le k_4 \le 330)$

$k_5 = 2500 \quad (2500 \le k_5 \le 6000)$

$k_6 = 2.2 \times 10^8 \quad (2.0 \times 10^8 \le k_6 \le 2.4 \times 10^8)$

$k_7 = 7 \times 10^{-2} \quad (0.0 \le k_7 \le 1)$

where TA, MOA, ETA, and P are tartronic acid, mesoxalic acid, 1,1,2,2-ethanetetracarbonic acid, and unspecified products, respectively. The rate equations were integrated numerically using the FACSIMILE program. The reaction scheme focuses on the key species of the investigated BZ subsystem, the aerobic oxidation of MA by Ce(IV). Besides MAOOH, which has been postulated, but not yet detected, the key intermediate MAOO• is experimentally shown to participate in the reaction. The rate constants k_1 and k_2 were determined by Försterling et al.[11] under nitrogen atmosphere, while no experimental data are available for the aerobic part of the model. Therefore, we adjusted these rate constants carefully in numerous simulations starting out from roughly estimated values given in refs 5 and 11–14 to fit the experimental decay curves. The fitting procedure is based on the minimization of the root-mean-square (RMS) deviation between the simulated and the measured peroxymalonyl radical decay. The error intervals of the rate constants (see reaction scheme) are also estimated from these RMS deviations. It may be noted that the rate constant for the production of MAOO•, k_3, is significantly slower than the diffusion-controlled limit.

Figure 2a shows the decay of the MAOO• and the (unscaled) oxygen concentration. After a fast increase in MAOO• concentration (0.3 s, not resolved in the experiment), two different phases of the decay can be distinguished. The first phase is characterized by a slow consumption of MAOO•, which is followed by a fast exponential decay of [MAOO•]. The experimental rate constant for the exponential part was found to be $k_{exp} = 1.8\ s^{-1}$. Preliminary amperometric measurements of the oxygen concentration under similar conditions revealed a decrease to less than 1% within 3–5 s, which approximately corresponds to the response time of the electrode. This fast decay is reproduced in our simulations, which show good agreement with the experiments, thus supporting our mechanistic model. It is noteworthy that the transition between the two phases of the MAOO• decay kinetics coincides with the complete consumption of oxygen. Therefore, oxygen is considered as the main switch between an aerobic and an anaerobic pathway in the concentration evolution of the MAOO•, as long as the initial concentration of Ce(IV) is sufficiently high to deplete the oxygen completely. The experimental rate constant k_{exp} describes therefore the overall decay kinetics of the peroxymalonyl radical in the anaerobic phase of the reaction.

Figure 2b presents the decay kinetics of the malonyl radical obtained from oxygen-equilibrated solutions. The corresponding numerical curve is superimposed and complemented by the calculated Ce(IV) kinetics. Under the given conditions, both decay functions obey first-order rate laws. Deviations from the exponential behavior of the Ce(IV) decay, due to the presence of oxygen, can be observed within the first few seconds of the simulation. The experimental rate constant for the MA• consumption is $k_{exp} = 0.062\ s^{-1}$ (within experimental error), which agrees well with the numerically obtained value of $k_{num} = 0.074\ s^{-1}$. We obtained $k_{num} = 0.148\ s^{-1}$ for the calculated rate constant of the reduction of Ce(IV), which is twice as large as the rate constant for the MA• consumption. For anaerobic conditions, a factor of 2.0 between these rate constants has been reported[8,13,14] and explained by Försterling et al.[9,14]

In conclusion, the measured decay kinetics of MA• as well as the MAOO• (Figure 2a,b) are consistent with our numerical result, that oxygen is consumed within the first seconds of the reaction. During this period a distinct aerobic pathway is observed. When oxygen is depleted, the reaction switches to an anaerobic pathway. This means that the intermediates which are directly produced by oxygen (MAOO• and MAOOH) are not able to maintain the reaction on the aerobic kinetic regime. Nevertheless, under initially aerobic conditions, it is highly probable that the oxygen-specific intermediates decay to products which are not formed under inert gas atmospheres. These products may account for long-term deviations between aerobically and anaerobically run BZ reactions.

Acknowledgment. This work was supported by an NSF-EPSCoR grant to R.H.S. and DOE/BOM Grant No. 1135142 and NIOSH Grant No. U60-CCU306149 to N.S.D.

JA9439175

(11) Försterling, H.-D.; Stuk, L. *J. Phys. Chem.* **1992**, *96*, 3067–3072.
(12) Pan, X.-M.; von Sonntag, C. *Z. Naturforsch.* **1990**, *45b*, 1337–1340.
(13) Försterling, H.-D.; Pachl, R.; Schreiber, H. *Z. Naturforsch.* **1987**, *42a*, 963–969.
(14) Försterling, H.-D.; Stuk, L. *J. Phys. Chem.* **1991**, *95*, 7320–7325. Försterling, H.-D.; Murányi, Sz. *Z. Naturforsch.* **1990**, *45a*, 1259–